

Surface Chemistry of Five-Membered Aromatic Ring Molecules Containing Two Different Heteroatoms on Si(111)-7 × 7

Feng Tao and Steven L. Bernasek*

Contribution from the Department of Chemistry, Princeton University,
Princeton, New Jersey, 08544

Received January 10, 2007; E-mail: sberna@princeton.edu

Abstract: The surface chemistry of three representative aromatic molecules containing two different heteroatoms isoxazole, oxazole, and thiazole on Si(111)-7 × 7 was studied. These molecules exhibit different competition and selectivity for multiple reaction channels with this surface, determined by a combination of molecular electronic and structural factors. Isoxazole is chemically attached to Si(111)-7 × 7 through both dative-bond addition and [4 + 2]-like cycloaddition. Oxazole chemisorbs on Si(111)-7 × 7 through both dative-bond addition and [2 + 2]-like cycloaddition. The kinetically favored [2 + 2]-like cycloadduct at low temperature is thermally converted into the thermodynamically preferred [4 + 2]-like cycloadduct at a temperature higher than 300 K. Thiazole is chemically bound to this surface only through formation of a Si···N dative bond at low temperature. This dative-bonded molecule is thermally converted into a [4 + 2]-like cycloadduct. The reaction channels of the three five-membered aromatic molecules containing two different heteroatoms (isoxazole, oxazole, and thiazole) and of the aromatic molecules containing only one heteroatom (pyridine, pyrrole, furan, and thiophene) are compared and analyzed for a thorough understanding of the reaction mechanisms of various heterocyclic aromatic molecules on this surface. The intrinsic connection between surface reaction mechanism and molecular electronic structure is demonstrated. This includes the distribution of electron density on the molecular ring determined by the geometric arrangement of the heteroatoms, the electronegativity of the heteroatoms, and the electronic contribution of the heteroatoms to formation of aromatic π conjugation, as well as the molecular polarity.

1. Introduction

Chemical attachment of organic molecules on semiconductor surfaces has attracted significant attention recently as the functionalized semiconductor surfaces exhibit promising applications in a wide spectrum of technological areas including micromechanical devices, biosensing techniques, and new-generation molecular electronic devices.^{1–5} Aromatic molecules are one of the main categories of organic molecules. They are important building blocks for many organic materials. The study of surface reactions of aromatic molecules on semiconductor surfaces is important for organic functionalization and modification of semiconductor surfaces. Surface reactions of simple aromatic molecules including benzene, pyridine, pyrrole, furan, and thiophene have been studied.^{1–12} However, a thorough

understanding of reaction mechanisms of various aromatic molecules on semiconductor surfaces is still lacking, particularly for complex multi-heteroatom aromatic systems.

The criterion for aromaticity was recognized by Huckel.¹³ An aromatic molecule is a cyclic planar molecule in which each atom of the molecular ring has one p orbital available for forming a set of molecular orbitals. For example, a cyclic planar molecule with a closed loop of 6, 10, 14, 18, and so on ($4n + 2$) π electrons in a fully conjugated ring is aromatic. Straightforwardly, to be an aromatic molecule, a molecule must (1) be cyclic, (2) have one available p orbital on each atom of the ring, (3) be planar or at least nearly planar so that there is continuous or nearly continuous overlap of all adjacent p orbitals of the ring, and (4) have a closed loop of ($4n + 2$) π electrons in the cyclic arrangement of p orbitals. The continuous π conjugation results in a resonance stabilization energy. This resonance energy makes the aromatic molecules prefer electrophilic substitution to electrophilic addition in solution-based organic reactions,^{13–15} which is distinctly different from the reactions observed on semiconductor surfaces.^{2–5}

- (1) Yates, J. T. *Science* **1998**, 279, 335–336.
- (2) Bent, S. F. *Prog. Surf. Sci.* **2003**, 73, 1–56.
- (3) Hamers, R. J.; Coulter, S. K.; Ellison, M. D.; Hovis, J. S.; Padowitz, D. F.; Schwartz, M. P.; Greenlief, C. M.; Russell, J. N. *Acc. Chem. Res.* **2000**, 33, 617–624.
- (4) Wolkow, R. A. *Annu. Rev. Phys. Chem.* **1999**, 50, 413–441.
- (5) Tao, F.; Xu, G. Q. *Acc. Chem. Res.* **2004**, 37, 882–893.
- (6) Taguchi, Y.; Fujisawa, M.; Nishijima, M. *Chem. Phys. Lett.* **1991**, 178, 363–368.
- (7) Cao, Y.; Wei, X. M.; Chin, W. S.; Lai, Y. H.; Deng, J. F.; Bernasek, S. L.; Xu, G. Q. *J. Phys. Chem. B* **1999**, 103, 5698–5702.
- (8) Kawasaki, T.; Sakai, D.; Kishimoto, H.; Akbar, A. A.; Ogawa, T.; Oshima, C. *Surf. Interface Anal.* **2001**, 31, 126–130.
- (9) Cao, Y.; Yong, K. S.; Wang, Z. H.; Chin, W. S.; Lai, Y. H.; Deng, J. F.; Xu, G. Q. *J. Am. Chem. Soc.* **2000**, 122, 1812–1813.

- (10) Cao, Y.; Wang, Z. H.; Deng, J. F.; Xu, G. Q. *Angew. Chem., Int. Ed.* **2000**, 39, 2740–2743.
- (11) Yuan, Z. L.; Chen, X. F.; Wang, Z. H.; Yong, K. S.; Cao, Y.; Xu, G. Q. *J. Chem. Phys.* **2003**, 119, 103891–10395.
- (12) Tao, F.; Lai, Y. H.; Xu, G. Q. *Langmuir* **2004**, 20, 366–368.
- (13) Sainbury, M. *Aromatic Chemistry*; Oxford University: Oxford, 1992.

The carbocyclic aromatic ring molecule is one type of aromatic molecule without any heteroatom. The simplest example is benzene, which in general is taken as a prototype of aromatic systems in various studies. In its hexagonal structure, each carbon atom with sp^2 hybridization is equivalent in electronic structure and chemical reactivity. Each of the six p orbitals on the molecular ring overlaps with its two neighbors, thereby forming a continuous π system and resulting in a resonance stabilization energy of ~ 150 kJ/mol.¹³ Benzene was the first aromatic molecule studied on Si(111)- 7×7 . The initial study proposed a π -binding mode based on electron energy loss spectroscopy (EELS).⁶ In that mode, the aromatic π system remains intact upon reaction. Recent vibrational studies using EELS with a higher resolution⁷ and scanning tunneling microscopy (STM)⁸ clearly show that benzene reacts with an adatom–rest atom pair on the Si(111)- 7×7 surface via a [4 + 2]-like cycloaddition and forms a 1,4-cyclohexadiene-like product bonded to the surface by breaking the aromatic π conjugation and producing two new Si–C σ bonds.

The majority of aromatic molecules contain one or more heteroatoms. These heterocyclic aromatic molecules can be categorized into three types:^{13–15} (1) where one heteroatom replaces a C=C unit of a carbocyclic aromatic molecule such as thiophene; (2) where one heteroatom only replaces one carbon atom such as pyridine; (3) where both of the two kinds of heteroatoms are present. The heteroatom of the first type provides two electrons for formation of the aromatic π system; however, the heteroatom of the second type provides only one electron for the aromatic π conjugation; they are simple aromatic molecules. The third type is the complex multi-heteroatom aromatic system.

Previous studies have mainly concerned simple aromatic molecules which contain only one heteroatom. Thiophene,⁹ furan,¹⁰ pyrrole,¹¹ and pyridine¹² are four important examples of simple aromatic molecules studied on Si(111)- 7×7 . These four simple heteroatom aromatic molecules exhibit significant differences in their reaction channels on Si(111)- 7×7 .^{9–12} However, there are very few studies addressing the driving force for the difference in reaction mechanisms of these aromatic molecules. Answering whether and how the distinctly different reaction pathways are determined by the intrinsic molecular and electronic structures has not been determined, though the chemical binding for each of these simple aromatic molecules has been studied. This is one of the issues to be addressed in this paper.

For complex multi-heteroatom aromatic molecules such as the third category described above, the different heteroatoms contribute distinctly differently in formation of the aromatic π conjugation. Three examples of these complex multi-heteroatom aromatic systems include isoxazole, oxazole, and thiazole. Each of the three molecules has two heteroatoms, a nitrogen atom and an oxygen atom (or sulfur atom). The oxygen or sulfur atom of these molecules provides two electrons from the unhybridized p orbital, and therefore, molecular aromatic π conjugation is partially contributed by delocalization of the unhybridized lone pair of the oxygen or sulfur atom. The nitrogen atom replaces one carbon atom, providing one electron for the aromatic π

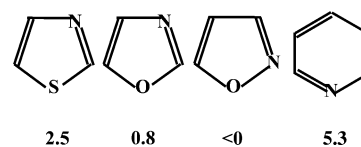


Figure 1. Basicity (shown with pK_a) of thiazole, oxazole, isoxazole, and pyridine.

system. Thus, it has one lone pair available for donation or protonation. Figure 1 lists the basicity of thiazole, oxazole, isoxazole, and pyridine (shown with pK_a). The basicity of oxazole ($pK_a = 0.8$)¹⁵ is weaker than thiazole ($pK_a = 2.5$)¹⁵ due to the stronger electron-withdrawing effect of the oxygen atom than the sulfur atom on the nitrogen in the ring. Compared to the nitrogen atom of oxazole, the nitrogen atom of isoxazole has a lower electron density and weaker basicity due to the stronger electron-withdrawing effect of the adjacent oxygen atom in this molecule compared to that from the internal oxygen atom in oxazole. Pyridine has a higher basicity than isoxazole, oxazole, and thiazole since there is no electron-withdrawing heteroatom such as oxygen or sulfur in the ring. The difference in basicity among the three molecules suggests that the distribution of electron density in a heteroatom aromatic molecule is dominated by several complex factors including the electronegativity of the heteroatoms, the geometric arrangement of the heteroatoms on the aromatic ring, and the electronic contribution of heteroatoms for formation of aromatic π conjugation.

It is expected that the molecular electronic distribution determines, or at least significantly impacts, the reaction mechanisms of these complex aromatic molecules. In order to demonstrate the intrinsic connection between reaction mechanism and these electronic and structural factors for various aromatic systems, three representative complex multi-heteroatom aromatic molecules, isoxazole, oxazole, and thiazole, were chosen for study. Each of the three molecules has two heteroatoms which are different in electronegativity, electronic contribution to formation of the aromatic π conjugation system, and even geometrical arrangement on the molecular ring. Thus, they are excellent systems for understanding the reaction mechanisms of complex multi-heteroatom aromatic molecules at the level of electronic structures and elucidating these intrinsic connections between reaction mechanism and these structural and electronic factors.

2. Experimental Section

The experiments were performed in a high-resolution electron energy loss spectrometer/ultrahigh vacuum (HREELS/UHV) system with a base pressure of 7.0×10^{-11} Torr. The UHV system is equipped with a HREELS spectrometer (LK3000-14R), low-energy electron diffraction (LEED) optics, and a mass spectrometer. This HREELS spectrometer consists of two 127° cylindrical deflector analyzers (CDAs) as the monochromator and two 127° CDAs for energy analysis. For HREELS measurement, an electron beam with a primary energy (E_p) of 5.0 eV collides with the sample surface at an incident angle (θ_i) of 60° from the surface normal. The energy resolution of the measured spectra indicated as full width at half-maximum (fwhm) was determined to be ~ 40 cm^{-1} . The Si(111) samples (9 mm \times 18 mm \times 0.38 mm) were cut from n-type (P-doped) silicon wafers with a purity of 99.999% (Goodfellow). A Ta foil with a thickness of 0.025 mm was sandwiched between two identical Si samples with a set of Ta clips and spot-welded to two Ta posts (diameter ≈ 1.5 mm) at the bottom of a Dewar-type liquid nitrogen-cooled sample holder. The sample was heated by

(14) Garratt, P. J. *Aromaticity*; McGraw-Hill: Maidenhead, U.K., 1971.

(15) Davies, D. T. *Aromatic Heteroatom Chemistry*; Oxford University: Oxford, 1992.

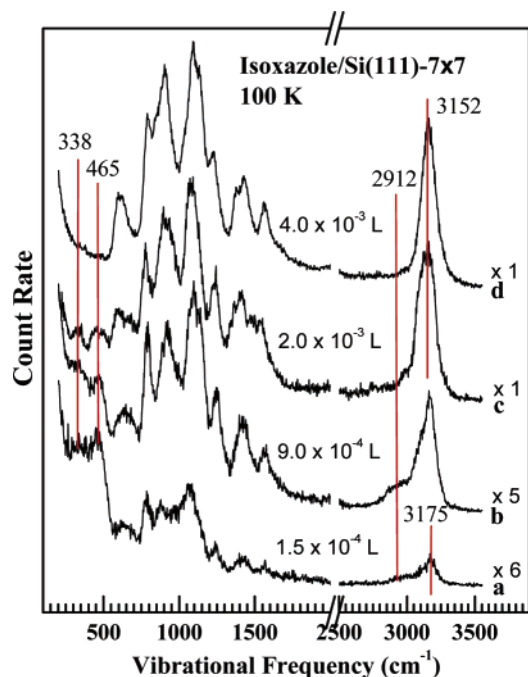


Figure 2. HREELS spectra of isoxazole adsorbed on a clean Si(111)-7 \times 7 at 100 K as a function of exposure.

resistive heating of the sandwiched Ta foil. It can be cooled to 95–100 K through the liquid nitrogen reservoir. Sample heating and cooling is precisely controlled by a temperature controller and an attached K-type thermocouple. After degassing the sample by annealing it at 850 K for 24 h the sample was carefully cleaned by cycles of Ar⁺ sputtering and annealing to 1200 K. A routine annealing procedure was carried out for formation of a 7 \times 7 reconstruction in UHV. Isoxazole (99%, Aldrich), oxazole (98%, Aldrich), and thiazole (99%, Aldrich) were further purified by several freeze–pump–thaw cycles before being dosed onto the Si(111)-7 \times 7 surface using a directed doser positioned in front of the sample. This doser was connected to a vapor introduction manifold through a Varian adjustable leak valve. The dosing tube had an internal diameter of \sim 7 mm and was positioned 2–3 mm from the sample surface. The exposures reported here were determined on the basis of the reading of the ion gauge without calibration remotely located in the UHV chamber and are quoted in Langmuir (1 L = 10⁻⁶ Torr s). The actual exposure at the surface from the directed doser is estimated to be 800–1000 times the reported exposure. Relative exposures can be compared in this data, but absolute values are not accurately available.

3. Results

3.1. Isoxazole on Si(111)-7 \times 7. Figure 2 shows the exposure-dependent vibrational spectra of isoxazole on Si(111)-7 \times 7 at 100 K. The vibrational features of the spectrum at high exposure (Figure 2d) match with the vibrational signature of liquid isoxazole¹⁶ very well. Spectra corresponding to exposures $< 2 \times 10^{-3}$ L as in Figure 2b are attributed to the chemisorbed molecules. At low exposure (Figure 2a and 2b), the vibrational features of the C–H stretching modes consist of a sharp peak at \sim 3175 cm⁻¹ and a small shoulder at \sim 2912 cm⁻¹. The shoulder at 2912 cm⁻¹ is absent in the spectrum at high exposure (Figure 2d). The vibrational feature at \sim 2912 cm⁻¹ definitely shows that a [4 + 2]- or [2 + 2]-like cycloadduct with one or more sp³-hybridized carbon atoms forms at 100 K. Compared

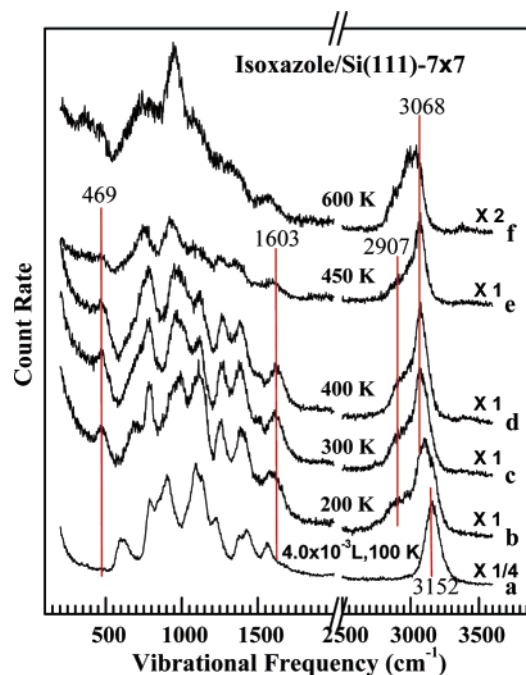


Figure 3. HREELS spectra of isoxazole adsorbed on Si(111)-7 \times 7 as a function of sample temperature.

to the spectrum at high exposure (4×10^{-3} L), two new peaks at \sim 338 and \sim 465 cm⁻¹ are observed in the spectra at lower exposures (Figure 2a–c). Thermal evolution in Figure 3 shows that no peak at \sim 338 cm⁻¹ for the chemisorbed monolayer is observed at a temperature higher than 200 K. Thus, the peak at \sim 338 cm⁻¹ is attributable to a relatively weakly chemisorbed species, a dative-bonded adduct at 100 K. This assignment will be discussed in section 4. The dative-bonded adduct and σ -bonded cycloadduct coexist at low temperature.

The spectrum of the physisorbed multilayer (curve a) is also shown in Figure 3 for comparison. Figure 3b is the spectrum of the chemisorbed molecules at 200 K. The spectrum at 200 K is similar to those seen at 300 and 400 K. However, the vibrational frequency of the C(sp²)–H stretching mode at 200 K is higher than that seen at 300 and 400 K. This difference possibly suggests that there is still a small amount of dative-bonded adduct at 200 K. The absence of an identifiable vibrational feature at \sim 338 cm⁻¹ for the Si \cdots N dative bond at 200 K may result from the small amount of the remaining dative-bonded molecules upon annealing to 200 K. In addition, the high baseline in the region of \sim 338 cm⁻¹ in Figure 3b overlaps the weak stretching mode of the Si \cdots N dative bond of the remaining dative-bonded species. Upon warming to 300 K, the C–H stretching peak shifts to \sim 3068 cm⁻¹. This indicates that the weakly dative-bonded molecules completely desorb or convert into σ -bonded cycloadduct at a temperature between 200 and 300 K.

The chemisorbed molecules at 300 K (Figure 3c) exhibit vibrational features significantly different from the physisorbed molecules at 100 K (Figure 3a). The shoulder at \sim 2907 cm⁻¹ of the chemisorbed molecules suggests that one or more carbon atoms rehybridize into sp³ due to [4 + 2]- or [2 + 2]-like cycloaddition. Figure 4 schematically presents three possible [4 + 2]- or [2 + 2]-like cycloadducts containing one C=C or C=N bond. Compared to the physisorbed multilayer, two new peaks at 469 and 1603 cm⁻¹ are observed in the spectrum of

(16) Ademברי, G.; Speroni, G.; Califano, S. *Spectrochim. Acta* **1963**, *19*, 1145–1152.

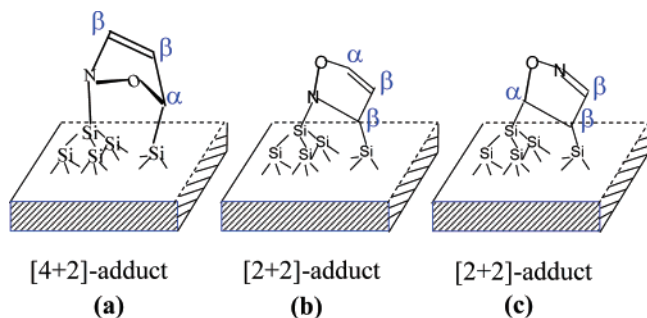


Figure 4. Three possible [4 + 2]- and [2 + 2]-like cycloadducts of isoxazole on Si(111)-7 × 7.

the chemisorbed molecules at 300 K (Figure 3c). The vibrational frequency at 1603 cm^{-1} is reasonably assigned to the C=C stretching mode of the *cis*-HRC=CHR skeleton.^{17,18} Thus, a [2 + 2]-like cycloaddition occurs at the C=C bond, and formation of a cycloadduct containing a C=N bond (Figure 4c) is precluded. Isoxazole could form a [4 + 2]- or [2 + 2]-like cycloadduct containing one C=C bond as shown in Figure 4a and 4b. Each of the two possible products bonds to the silicon surface through both Si-C and Si-N σ bonds. The peak at $\sim 469 \text{ cm}^{-1}$ in Figure 3c is assigned to the Si-C stretching mode based on the observed Si-C stretching at $\sim 450 \text{ cm}^{-1}$ for chemisorbed ethylene on Si(100)¹⁹ and $\sim 540 \text{ cm}^{-1}$ for chemisorbed benzene on Si(111)-7 × 7.¹⁰ The Si-N stretching mode of the chemisorbed molecules usually appears in a region lower than 1000 cm^{-1} .²⁰ Here it is difficult to differentiate the Si-N stretching from other modes in this vibrational region.

Identification of the product from two possible cycloadducts (Figure 4a and 4b) is challenging. Until now, almost all studied conjugated dienes have been chemically bound to Si(111)-7 × 7 through a [4 + 2]-like cycloaddition mechanism at a relatively high-temperature such as 300–400 K.⁵ This is because the large spatial distance between an adatom and its neighboring rest atom, 4.53 Å, makes the [4 + 2]-like cycloadduct favorable thermodynamically. In addition, the [4 + 2]-like cycloaddition is also a kinetically favorable pathway for isoxazole on Si(111)-7 × 7 (see section 4). From this point, we may possibly assign the [4 + 2]-like cycloadduct (Figure 4a) as the product of isoxazole on Si(111)-7 × 7 at 200–450 K. On the other hand, if we consider that the two possible [4 + 2]- and [2 + 2]-like cycloadducts in Figure 4a and 4b are analogous to 2,5-dihydrofuran and 2,3-dihydrofuran, respectively, then the C-H vibrational features of the formed cycloadduct of isoxazole support the assignment of the [4 + 2]-like cycloadduct (see Supporting Information).

3.2. Oxazole on Si(111)-7 × 7. **3.2.1. Dative-Bond Addition and [2 + 2]-like Cycloaddition at Low Temperature.** Figure 5 is the vibrational spectra of oxazole on Si(111)-7 × 7 at 100 K as a function of molecular exposure. Obviously, the high exposure forms a physisorbed multilayer with the same vibrational signature as liquid oxazole.²¹ Notably, the C-H vibra-

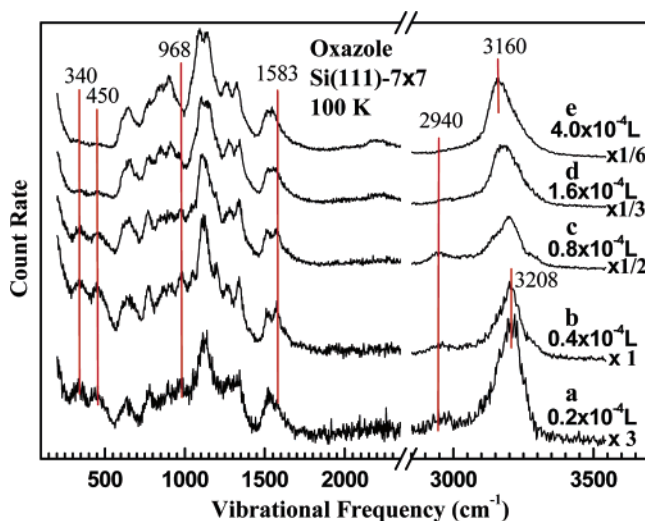


Figure 5. HREELS spectra of oxazole adsorbed on a clean Si(111)-7 × 7 at 100 K as a function of exposure.

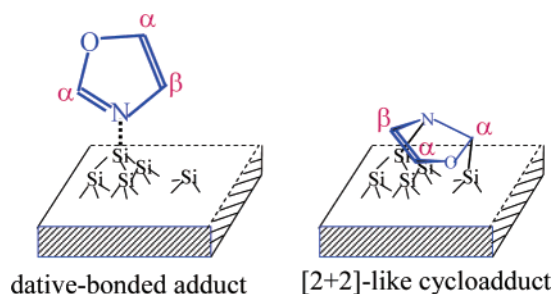


Figure 6. Schematics of dative-bonded adduct and [2 + 2]-like cycloadduct of oxazole formed at 100 K on Si(111)-7 × 7.

tional features at low exposures are different from those at high exposures. A peak at $\sim 2940 \text{ cm}^{-1}$ clearly appears at low exposures, suggesting that one or more carbon atoms rehybridize into sp^3 due to a [4 + 2]- or [2 + 2]-like cycloaddition. The occurrence of the [4 + 2]- or [2 + 2]-like cycloaddition is also supported by the appearance of a new peak at $\sim 1583 \text{ cm}^{-1}$ attributed to a C=X (X = C or N) stretching mode²² in Figure 5a–c. The spectra at low exposures (Figure 5a, 5b, and 5c) have three new peaks at ~ 340 , ~ 450 , and $\sim 968 \text{ cm}^{-1}$, in contrast to the physisorbed molecules. The low vibrational frequency at $\sim 340 \text{ cm}^{-1}$ suggests formation of a dative-bonded adduct since the nitrogen atom of oxazole has one localized lone pair. Referring to the vibrational frequency of the Si-C bond of the cycloadduct of isoxazole and the Si-N bond of the dissociated product of ammonia on Si(111)-7 × 7,²⁰ the new peaks of 450 and 968 cm^{-1} for the chemisorbed molecules at low temperature are assigned to this Si-C and Si-N stretching, respectively. This assignment suggests formation of a [2 + 2]-like cycloadduct containing a C=C bond. Therefore, oxazole forms both dative-bonded adduct and [2 + 2]-like cycloadduct at low temperature as illustrated in Figure 6.

3.2.2. Thermal Evolution and the Thermally Driven Switch of Binding Configuration of Oxazole. Figure 7 presents the vibrational features of the chemisorbed oxazole molecules as a function of sample temperature. Figure 7a is the vibrational spectrum of the chemisorbed molecules at 100 K. When the

(17) Socrates, G. *Infrared Characteristic Group Frequencies*; John Wiley & Sons: Chichester, 1980.

(18) Dollish, F.; Fateley, W. G.; Bentley, F. F. *Characteristic Raman Frequencies of Organic Compounds*; John Wiley & Sons: New York, 1974.

(19) Widdra, W.; Huang, C.; Briggs, G. A. D.; Weinberg, W. H. *J. Electron. Spectrosc. Relat. Phenom.* **1993**, *64–65*, 129–136.

(20) Colaianni, M. L.; Chen, P. L.; Yates, J. T. *J. Chem. Phys.* **1992**, *96*, 7826–7837.

(21) Sbrana, G.; Castellucci, E.; Ginanneschi, M. *Spectrochim. Acta* **1967**, *23A*, 751–758.

(22) Daimay, L. V.; Norman, B. C.; William, G. F.; Jeanette, G. G. *The Handbook of Infrared and Raman Characteristic Frequency of Organic Molecules*; Academic Press: Boston, 1991.

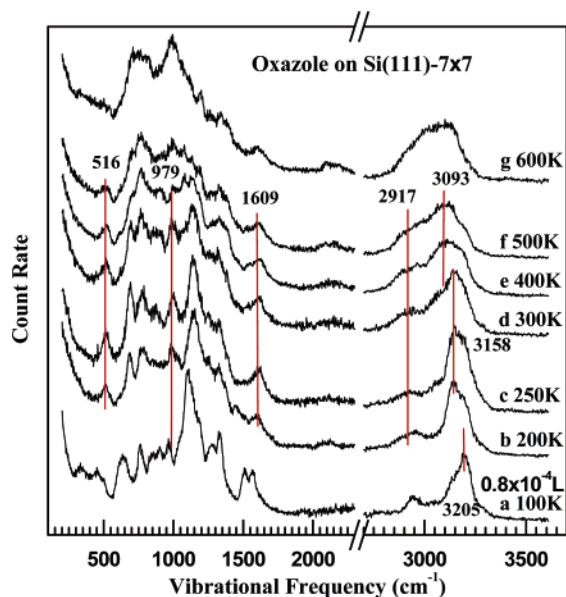


Figure 7. HREELS spectra of oxazole adsorbed on Si(111)-7 × 7 as a function of sample temperature.

sample is warmed to 200 K, there are some changes to the vibrational features. First, the peak for C(sp²)-H red shifts to ~3158 cm⁻¹, though there is still some contribution from the C-H vibration at ~3205 cm⁻¹. This suggests that the dative-bonded adduct does not completely desorb or is not completely converted into cycloadduct. Compared to Figure 7a, the second change is the appearance of a new peak at ~516 cm⁻¹. The third change is the significant weakening or even disappearance of the stretching mode of the Si...N dative bond at ~340 cm⁻¹.

At 200–300 K, the vibrational peaks at ~516 and ~979 cm⁻¹ can be assigned to the Si-C^{7,19} and Si-N²⁰ σ bonds, suggesting preservation of the [2 + 2]-like cycloadduct formed at 100 K. The vibrational feature for C(sp²)-H stretching at ~3158 cm⁻¹ is consistent with that of liquid 2,3-dihydrofuran,²³ further supporting formation of the [2 + 2]-like cycloadduct in this temperature range. In addition, the vibrational frequency of the α -C(sp²)-H mode in the [2 + 2]-like cycloadduct of oxazole (~3158 cm⁻¹ in Figure 7b) is higher than that of the β -C(sp²)-H mode in the [4 + 2]-like cycloadduct of isoxazole (~3068 cm⁻¹ in Figure 3c). This difference between the α -C(sp²)-H vibrational frequency of the [2 + 2]-like cycloadduct of oxazole and the β -C(sp²)-H vibrational frequency of the [4 + 2]-like cycloadduct of isoxazole is consistent with the higher vibrational frequency of α -C(sp²)-H stretching in 2,3-dihydrofuran in contrast to the β -C(sp²)-H vibrational frequency of 2,5-dihydrofuran.^{23–25} This comparison further confirms the assignment of the [4 + 2]-like cycloadduct for isoxazole and [2 + 2]-like cycloadduct for oxazole, respectively.

Compared to the vibrational features at 300 K, some new vibrational features appear at 400 and 500 K. First, the peak for the C-H stretch red shifts. Second, the vibrational feature of the Si-N σ bond is weakened on heating from 400 to 500 K, though there is no obvious change in the intensity of the vibrational feature of the Si-C stretching mode at ~516 cm⁻¹. Upon annealing at 500 K, the peak of the C(sp²)-H stretching

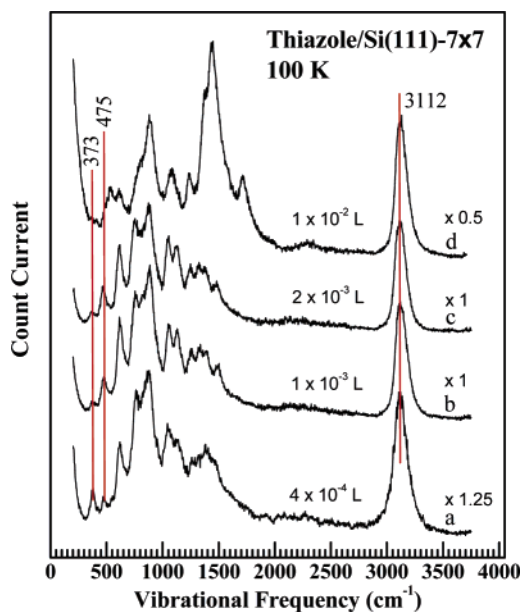


Figure 8. HREELS spectra of thiazole adsorbed on a clean Si(111)-7 × 7 at 100 K as a function of exposure.

mode red shifts to 3093 cm⁻¹. This vibrational frequency is in agreement with that of the C(sp²)-H stretching mode of liquid 2,5-dihydrofuran,²³ indicating that the [2 + 2]-cycloadduct is possibly partially converted into a [4 + 2]-cycloadduct. The red shift of the C(sp²)-H vibrational frequency is in good agreement with formation of a [4 + 2]-like cycloadduct in this temperature range, as the formed [4 + 2]-like cycloadduct does not have an α -C(sp²)-H bond with high C-H stretching frequency, while there is such a bond in the [2 + 2]-like cycloadduct. Thus, the temperature-dependent change of vibrational frequency suggests a thermally driven switch of the molecular binding configuration.

3.3. Thiazole on Si(111)-7 × 7. 3.3.1. Evidence for Dative-Bond Addition at Low Temperature. Figure 8 presents the vibrational spectra of thiazole adsorbed on Si(111)-7 × 7 with different exposures at 100 K. Molecular vibrational features at high exposure (1.0 × 10⁻² L, Figure 8d) are in good agreement with the vibrational signature of liquid thiazole.²¹ However, the vibrational spectra at low exposures (Figure 8a–c) are different from that of the physisorbed multilayer (Figure 8d). The vibrational peak at ~373 cm⁻¹ is absent in the spectra of the physisorbed molecules. Thus, it is assigned to the chemisorbed molecules. The chemisorbed molecules contribute to the spectra of Figure 8a–c to different extents. The vibrational feature of the C-H stretching mode appears as a symmetric sharp peak centered at ~3112 cm⁻¹. Notably, there is no identifiable change in the C-H stretching mode with the increase of exposure in Figure 8, suggesting that neither the [4 + 2]- nor the [2 + 2]-like cycloadduct is formed at this temperature.

For isoxazole and oxazole, formation of [4 + 2]- or [2 + 2]-like cycloadduct at 100 K is clearly evidenced by the appearance of a shoulder at 2900–2950 cm⁻¹ attributed to the C(sp³)-H stretching mode. However, no identifiable vibrational feature at 2900–2950 cm⁻¹ can be found for the chemisorbed thiazole at 100 K, suggesting the absence of cycloadduct at low temperature. Notably, although the vibrational features at ~465 cm⁻¹ for the [4 + 2]-like cycloadduct of isoxazole (Figure 2) and ~450 cm⁻¹ for [2 + 2]-like cycloadduct of oxazole (Figure

(23) Klotz, T. D.; Collier, W. B. *Spectrochim. Acta A* **1994**, *50*, 1725–1748.

(24) Green, W. H.; Harvey, A. B. *Spectrochim. Acta A* **1969**, *25*, 723–730.

(25) ElAzhary, A. A.; Hilal, R. H. *Spectrochim. Acta A* **1997**, *53*, 1365–1373.

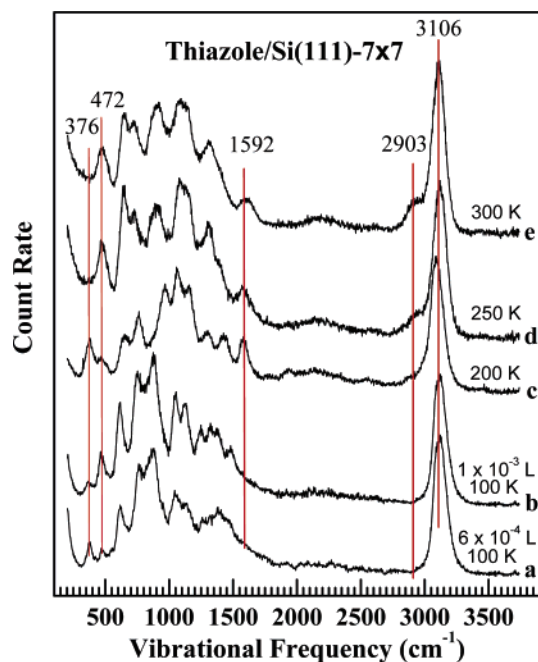


Figure 9. HREELS spectra showing the thermal conversion of dative-bonded adduct of thiazole into [4 + 2]-like cycloadduct.

5) were assigned to Si–C stretching modes, the vibrational peak at ~ 475 cm^{-1} for the adsorbed thiazole at 100 K cannot be assigned to the Si–C stretching mode since there is no evidence for a [4 + 2]- or [2 + 2]-like cycloadduct formed at this temperature. Alternatively, the peak at ~ 475 cm^{-1} is attributed to the ring vibrational mode²⁶ as formation of a Si \cdots N dative bond does not break the aromatic ring, though the dative-bond addition possibly influences the distribution of electron density on the molecular ring to some extent.

3.3.2. Conversion of Dative-Bonded Adduct into Covalent-Bonded Cycloadduct. Figure 9a and 9b presents the spectra for 6×10^{-4} and 1×10^{-3} L exposure of thiazole, respectively. Figure 9c, 9d, and 9e shows the spectra obtained by annealing the sample exposed to 1×10^{-3} L thiazole to 200, 250, and 300 K, respectively. Among the four spectra (Figure 9a–d), the relative intensities of the peaks at ~ 376 and ~ 472 cm^{-1} are different. Compared to the spectra for 6×10^{-4} L (Figure 9a), the intensity of the peaks at ~ 376 cm^{-1} attributed to the Si \cdots N dative bond and ~ 472 cm^{-1} corresponding to the molecular ring vibration decreases and increases simultaneously in the spectrum for 1×10^{-3} L (Figure 9b), respectively. This difference suggests that the physisorbed molecules cover the chemisorbed molecules (actually the dative-bonded molecules) and thereby weaken the HREELS signal of the dative-bonded monolayer. Compared to the spectrum for 1×10^{-3} L at 100 K, the intensity ratio between ~ 376 and ~ 472 cm^{-1} reverses in the spectrum at 200 K (Figure 9c). This is because desorption of physisorbed molecules from 100 to 200 K exposes the chemisorbed monolayer, producing a strong signal from the dative-bonded molecules. The re-appearance of the peak at ~ 376 cm^{-1} attributed to the Si \cdots N dative bond upon annealing from 100 to 200 K shows that at least a portion of the dative-bonded molecules is thermally stable at 200 K. On the other hand, the appearance of a new peak at ~ 1592 cm^{-1} attributed to C=C

stretching at 200 K suggests formation of a [4 + 2]- or [2 + 2]-like cycloadduct, further supported by the appearance of a small shoulder at ~ 2903 cm^{-1} at 200 K. Thus, the vibrational features at 200 K show the coexistence of dative-bonded adduct and cycloadduct.

As there is no [4 + 2]- or [2 + 2]-like cycloadduct formed at 100 K, the cycloadduct observed at 200 K definitely results from the thermally driven conversion of some of the dative-bonded adduct formed at 100 K. The intensity of the peak at ~ 472 cm^{-1} in the spectrum at 200 K is possibly contributed by the ring vibrational mode of the remaining dative-bonded adduct. In addition, it is possibly partially due to the stretching mode of the Si–C bond of the [4 + 2]- or [2 + 2]-like cycloadduct of thiazole at 200 K since the vibrational features of the Si–C stretching mode of cycloadducts of isoxazole and oxazole were observed at 450–516 cm^{-1} . The contribution of the Si–C stretching mode for the vibrational feature at ~ 472 cm^{-1} at 200 K is further supported by observation of a similar peak at ~ 472 cm^{-1} in the spectra of the chemisorbed layer without dative-bonded adduct at a higher temperature such as 250 and 300 K (Figure 9d and 9e). Compared to the spectrum at 200 K, the peak at ~ 376 cm^{-1} disappears and the intensity of the peak at ~ 472 cm^{-1} greatly increases in the spectrum at 250 K. This suggests that the dative-bonded molecules are completely converted into a [4 + 2]- or [2 + 2]-like cycloadduct at 250 K. Due to this conversion, the intensity of the shoulder at ~ 2903 cm^{-1} attributed to the C(sp³)–H stretching mode at 250 K is much larger than that at 200 K. The vibrational features at 250 K are very similar to those at 300 K, suggesting they are the same cycloadduct. At a temperature higher than 400 K, the cycloadduct starts to decompose on Si(111)-7 \times 7 (spectra not shown).

It should be noted that the vibrational frequency of the C–H stretching mode of physisorbed thiazole is lower than that of oxazole due to the stronger electron-withdrawing ability of the oxygen atom than the sulfur atom. The impact of the electron-withdrawing effect of oxygen (or sulfur) on the C–H stretching frequency is effective and significant due to molecular aromatic conjugation. However, for cycloadducts of these aromatic molecules, the aromatic conjugation is broken. Thus, the difference in the electron-withdrawing ability between oxygen atom in the cycloadducts of oxazole and sulfur atom in the cycloadduct of thiazole will have a much smaller impact on the α -(sp²)C–H stretching frequency in the cycloadducts. Considering the similarity of molecular structure between thiazole and oxazole, we can deduce the structure of the cycloadduct by comparing the frequency of the C(sp²)–H stretching mode of the cycloadduct of thiazole (Figure 9d and 9e) to those of the [4 + 2]- and [2 + 2]-like cycloadduct of oxazole. The vibrational frequency of ~ 3106 cm^{-1} for the C(sp²)–H of the chemisorbed thiazole at 250 and 300 K is consistent with ~ 3093 cm^{-1} of the [4 + 2]-like cycloadduct of oxazole on Si(111)-7 \times 7. It possibly indicates that the cycloadduct of thiazole on Si(111)-7 \times 7 is the preferred cycloadduct. However, since the difference in the electron-withdrawing ability of oxygen and sulfur atoms in these cycloadducts will still have an impact on the α -(sp²)C–H stretching frequency, we cannot completely preclude the possibility of a [2 + 2]-like cycloadduct of thiazole forming at 250–300 K.

(26) Sbrana, G.; Castellucci, E.; Ginanneschi, M. *Spectrochim. Acta A* **1967**, *23*, 751–758.

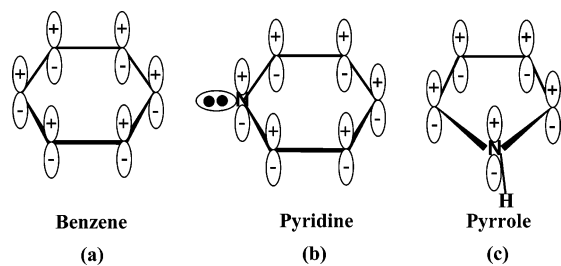


Figure 10. (a–c) Overlap of all parallel p orbitals and formation of the aromatic π conjugation of benzene, pyridine, and pyrrole.

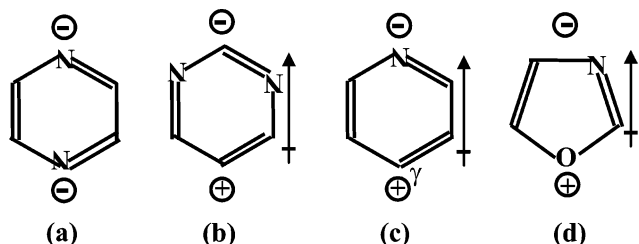


Figure 11. Polarity of pyrazine (a), pyrimidine (b), pyridine (c), and oxazole (d).

4. Discussion

A thorough understanding of the intrinsic factors determining reaction mechanisms of aromatic systems on $\text{Si}(111)\text{-}7 \times 7$ begins with interpreting the structural and electronic factors and reaction mechanisms of simple aromatic molecules including benzene, pyridine, pyrrole, thiophene, and furan. Figure 10 presents the $p\pi$ atomic orbitals of benzene, pyridine, and pyrrole.¹⁵ In benzene, every carbon atom is equivalently sp^2 hybridized. Three sp^2 orbitals of each carbon atom form three σ bonds with the two adjacent carbon atoms and one hydrogen atom. The unhybridized p orbital with one electron conjugates with the other five p orbitals, forming an aromatic sextet. Benzene is chemically attached to $\text{Si}(111)\text{-}7 \times 7$ via a [4 + 2]-like cycloaddition, forming a 1,4-cyclohexadiene-like cycloadduct. In pyridine, the nitrogen atom is unequivocally sp^2 hybridized. The remaining unhybridized p orbital of the nitrogen atom has one electron which combines with the other five p orbitals of the carbon atoms to form a conjugated sextet. Two sp^2 orbitals with one electron in each form two σ bonds with two carbon atoms. Notably, one sp^2 orbital has a lone pair which does not participate in the aromatic π -conjugation system. Thus, the nitrogen atom of pyridine is electron rich. However, the sp^2 hybridization of the nitrogen atom on pyrrole is different from that of pyridine. Its three sp^2 -hybridized orbitals are equivalent, forming two N–C bonds and one N–H bond. The unhybridized p orbital with a lone pair participates in the aromatic π conjugation, forming a sextet. Compared to the electron-rich nitrogen atom of pyridine, the nitrogen atom of pyrrole is relatively electron deficient due to the delocalization of the lone pair of the nitrogen atom on the aromatic ring of pyrrole.

The electron-rich nitrogen atom of pyridine can partially donate electron density to the electron-deficient adatom site of $\text{Si}(111)\text{-}7 \times 7$, forming a dative bond at the organic–semiconductor interface.¹² Thus, pyridine can be chemically bound to $\text{Si}(111)\text{-}7 \times 7$ through a $\text{Si}\cdots\text{N}$ dative bond.¹² However, pyrrole bonds to the $\text{Si}(111)\text{-}7 \times 7$ surface through N–H dissociation, not through an addition pathway.¹¹ The

product of this dissociation channel retains the aromatic pyrrolyl ring on this surface. Similar to pyrrole, the lone pair on the sulfur atom of thiophene and the oxygen atom of furan participates in formation of the six-electron aromatic π conjugation. Both thiophene and furan can be chemically attached to this surface through a stepwise radical mechanism, forming covalent-bonded cycloadducts.^{9,10} Besides the [4 + 2]-like cycloadduct, furan forms a dimerized adduct¹⁰ which is absent for thiophene on $\text{Si}(111)\text{-}7 \times 7$. This is possibly associated with the higher energy barrier of the transition state for the [4 + 2]-like cycloaddition of furan than for that of thiophene.^{9,10} This difference in energy barrier is expected from the higher thermal desorption temperature of the [4 + 2]-like cycloadduct of thiophene in contrast to that of furan. The higher energy barrier for [4 + 2]-like cycloaddition of furan possibly drives the mono- σ -bonded precursor to dimerize.¹⁰ However, a low-energy barrier makes the mono- σ -bonded precursor of thiophene only form a [4 + 2]-like cycloadduct on $\text{Si}(111)\text{-}7 \times 7$. Adsorption of pyridine, pyrrole, and thiophene on $\text{Si}(100)$ ^{27–31} results in the same product as adsorption of these molecules on the $\text{Si}(111)\text{-}7 \times 7$. For furan, however, only the [4 + 2]-like cycloadduct is seen on $\text{Si}(100)$.³² It should also be noted that thiophene can form a dative bond with $\text{Ge}(100)$,^{33,34} in contrast to the [4 + 2]-like cycloaddition observed on $\text{Si}(111)\text{-}7 \times 7$ ⁹ and $\text{Si}(100)$.³¹ This may result from the different electron density of the surface electron-deficient atoms of the $\text{Ge}(100)$ surface compared to $\text{Si}(111)\text{-}7 \times 7$ and $\text{Si}(100)$.

All three complex aromatic molecules (isoxazole, oxazole, and thiazole) belong to the category of aromatic molecule containing multi-heteroatoms in which an oxygen or a sulfur atom replaces two carbon atoms of benzene and a nitrogen atom replaces one carbon atom. The oxygen/sulfur atom and nitrogen atom contribute two and one electrons, respectively, for formation of an aromatic π conjugation of $4n + 2$ electrons. Compared to the two heteroatoms separated by carbon in oxazole, the two heteroatoms in isoxazole are adjacent. This geometric difference results in a different distribution of electron density on the molecular ring. In addition, the different heteroatoms in oxazole and thiazole also induce a different distribution of electron density.

As described in the Introduction, isoxazole has two heteroatoms with different electronic structures. Similar to pyridine, the lone pair of the nitrogen atom in isoxazole does not participate in formation of the aromatic π conjugation, though the lone pair is slightly withdrawn by its neighboring oxygen atom. Therefore, the lone pair of the nitrogen atom of isoxazole is still localized. The nitrogen atom of isoxazole has an electron density higher than the oxygen atom and all the carbon atoms of this molecule. Thus, the nitrogen atom can act as an electron donor. On the other hand, for $\text{Si}(111)\text{-}7 \times 7$ its adatom and

(27) Tao, F.; Qiao, M. H.; Wang, Z. H.; Xu, G. Q. *J. Phys. Chem. B* **2003**, *107*, 6384–6390.

(28) Qiao, M. H.; Tao, F.; Cao, Y.; Xu, G. Q. *Surf. Sci.* **2003**, *544*, 285–294.

(29) Wang, G. T.; Mui, C.; Tannaci, J. F.; Filler, M. A.; Musgrave, C. B.; Bent, S. F. *J. Phys. Chem. B* **2003**, *107*, 4982–4996.

(30) Cao, X.; Coulter, S. K.; Ellison, M. D.; Liu, H.; Liu, J.; Hamers, R. J. *J. Phys. Chem. B* **2001**, *105*, 3759–3768.

(31) Qiao, M. H.; Cao, Y.; Tao, F.; Liu, Q.; Deng, J. F.; Xu, G. Q. *J. Phys. Chem. B* **2000**, *104*, 11211–11219.

(32) Qiao, M. H.; Tao, F.; Cao, Y.; Li, Z. H.; Dai, W. L.; Deng, J. F.; Xu, G. Q. *J. Chem. Phys.* **2001**, *114*, 2766–2774.

(33) Jeon, S. M.; Jung, S. J.; Lim, D. K.; Kim, H. D.; Lee, H.; Kim, S. *J. Am. Chem. Soc.* **2006**, *128*, 6296–6297.

(34) Jeon, S. M.; Jung, S. J.; Kim, H. D.; Lim, D. K.; Lee, H.; Kim, S. *J. Phys. Chem. B* **2006**, *110*, 21728–21734.

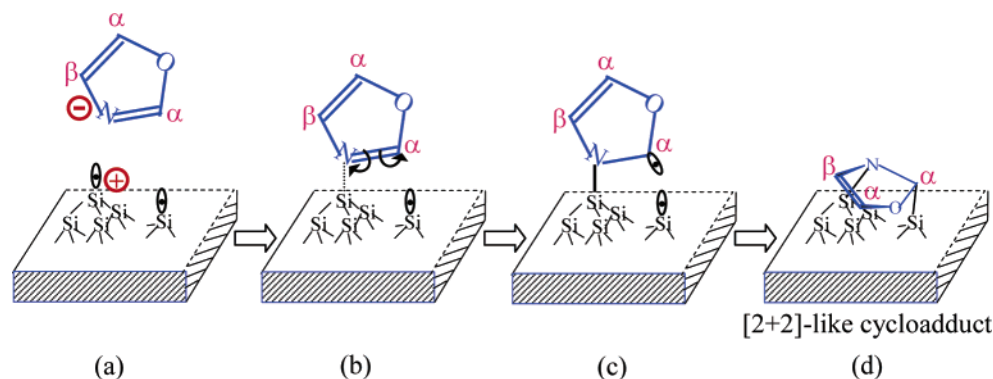


Figure 12. Pathway for formation of the [2 + 2]-like cycloadduct of oxazole on Si(111)-7 × 7.

rest atom are electron deficient and electron rich, respectively, due to a rearrangement of atom spatial positions and a complex redistribution of electron density during the 7 × 7 reconstruction.⁵ Thus, vibrational features at ~338 cm⁻¹ can be attributed to the Si···N dative bond formed between the electron-deficient adatom of Si(111)-7 × 7 and the electron-rich nitrogen atom of isoxazole.

Oxazole is an isomer of isoxazole. Their difference is the geometry of the nitrogen atom on the five-membered ring. For isoxazole, the nitrogen atom is adjacent to the oxygen atom. However, it is one atom distant from the oxygen atom in oxazole. The difference in heteroatom distribution on the aromatic ring gives rise to a difference in the distribution of electron density for the two molecules. The electron-withdrawing effect of oxygen for the nitrogen atom in oxazole is weaker than that for the case of isoxazole. Therefore, the nitrogen atom of oxazole has an electron density similar to that of pyridine, implying capability for a significant donation of electron density. Similar to oxazole, thiazole also exhibits the capability of donating electron density to form a Si···N dative bond.

Molecular polarity is possibly another necessary factor for formation of a dative bond between aromatic molecules and semiconductor surfaces. Pyrazine is a six-membered aromatic ring molecule with two symmetrically arranged nitrogen atoms (Figure 11a). Similar to the role of the nitrogen atom of isoxazole, oxazole, thiazole, and pyridine in formation of aromatic π conjugation, each nitrogen atom in pyrazine contributes only one electron for formation of the aromatic π sextet. Thus, each of the two nitrogen atoms in pyrazine has a high electron density due to their localized lone pairs. However, pyrazine does not form a dative bond with the Si(111)-7 × 7³⁵ and Si(100)³⁶ surfaces. This is possibly because the nonpolar pyrazine does not allow electron-rich nitrogen atoms to transfer electron density to the electron-deficient surface silicon atoms of Si(111)-7 × 7 and Si(100). This understanding is further supported by formation of a dative bond between pyrimidine (Figure 11b), an isomer of pyrazine with polarity, on Ge(100).³⁷ Thus, it is expected that polar pyrimidine possibly forms a dative bond with Si(100), Si(111)-7 × 7, and Ge(100). In addition, this understanding of the role of the molecular dipole is consistent with formation of dative bonds between oxazole,

isoxazole, thiazole, and Si(111)-7 × 7. All three molecules have a strong dipole moment. For example, oxazole has a stronger dipole than pyridine. This is because when compared to pyridine the oxygen side of oxazole is a stronger positive pole than C γ of pyridine due to the contribution of a lone pair from the oxygen atom to the other four atoms for formation of the aromaticity in oxazole (Figure 11c and 11d).

The lone pair in an unhybridized p orbital contributed by the oxygen atom of oxazole in fact plays a different role in formation of the aromatic π conjugation in contrast to the two electrons in two p orbitals of two carbon atoms in a pyridine molecule. To some extent, oxazole may be considered as a hybrid of furan and pyridine. In fact, oxazole can be chemically attached to Si(111)-7 × 7 through both the cycloaddition channel similar to thiophene and furan as well as the dative-bond addition similar to pyridine. Oxazole carries out the cycloaddition reaction at low temperature via a [2 + 2]-like cycloaddition, not a [4 + 2]-like cycloaddition. This is determined by its characteristic electronic structure. It is understandable if we consider this cycloaddition reaction as a stepwise reaction mechanism as schematically shown in Figure 12. Attack of a nitrogen atom on an adatom forms an intermediate with a lower energy than other possible intermediates because the nitrogen atom and silicon adatom are electron rich and electron deficient, respectively, and geometrically the adatom is at a favorable outward position in contrast to the inward rest atom. In addition, absorption of the radical of an electron-rich rest atom by an α -C atom with lower electron density due to the electron-withdrawing effect of its adjacent oxygen atom (Figure 12c) will facilitate subsequent formation of a Si–C σ bond. Therefore, [2 + 2]-like cycloaddition is a kinetically favorable pathway for oxazole at low temperature. For pyridine, however, the electron density of its α -C atom is not lower than that of its γ -C atom. Therefore, the [2 + 2]-like cycloaddition of pyridine is not kinetically favored. For isoxazole, an isomer of oxazole, its electron-rich nitrogen atom can form an intermediate with the electron-deficient adatom of Si(111)-7 × 7. Its α -C atom with lower electron density than the β -C atom due to the strong electron-withdrawing effect of the oxygen atom on its adjacent α -C atom can absorb the radical of the rest atom of this surface, forming a Si–C σ bond. Thus, the low electron density and favorable geometric arrangement of the α -C atom of isoxazole makes [4 + 2]-like cycloaddition thermodynamically and kinetically favorable.

Chemisorption of thiazole on Si(111)-7 × 7 is different from the simultaneous dative-bonded addition and [4 + 2]- or [2 +

(35) Huang, H. G.; Huang, J. Y.; Ning, Y. S.; Xu, G. Q. *J. Chem. Phys.* **2004**, *121*, 4820–4825.

(36) Huang, H. G.; Wang, Z. H.; Xu, G. Q. *J. Phys. Chem. B* **2004**, *108*, 12560–12567.

(37) Lee, Y.; Jung, S. J.; Hong, S.; Kim, S. J. *Phys. Chem. B* **2005**, *109*, 348–351.

2]-like cycloaddition for isoxazole and oxazole at low temperature. This difference can be understood in the contrast of their electronic structures. For both isoxazole and oxazole, the α -C atom has a low electron density due to the electron-withdrawing effect of the electronegative oxygen atom. Thus, for isoxazole the binding between the electron-rich N atom and the electron-deficient α -C atom and the adatom–rest atom pair of Si(111)-7 \times 7 is thermodynamically and kinetically favorable; for oxazole the attachment of the electron-rich N atom and the electron-deficient α -C to the adatom–rest atom pair is kinetically favorable at low temperature. Compared to isoxazole and oxazole, the α -C atom of thiazole has a relatively high electron density due to the absence of a strong electron-withdrawing effect from the sulfur atom with a relatively lower electronegativity than the oxygen atom. Thus, referring to the [2 + 2]-like cycloaddition of oxazole at low temperature (Figure 6b), for thiazole a chemical binding between the nitrogen atom and the α -C atom of thiazole and the adatom–rest atom pair to form a [2 + 2]-like cycloadduct is neither kinetically nor thermodynamically favorable. Alternatively, dative-bond addition between the electron-rich nitrogen atom of thiazole and the electron-deficient adatom site is kinetically favorable at low temperature.

Overall, the competition and selectivity of these reaction channels of each multi-heteroatom aromatic system is definitely dominated by the distribution of electronic density on the molecular ring, the geometric arrangement of heteroatoms on the ring, the electronegativity of the heteroatoms, and the molecular polarity.

5. Summary

The chemical attachment mechanisms of three complex five-membered aromatic molecules with two different heteroatoms were studied with the purpose of establishing the intrinsic connection *between* molecular electronic density, geometric arrangement, and electronegativity of heteroatoms, along with molecular polarity and aromaticity, *and* their reaction channels

on the Si(111)-7 \times 7 surface. The lone pair of one unequivalently hybridized p orbital of the nitrogen atom of the three molecules offers the capability of forming a dative bond with Si(111)-7 \times 7 due to the localized nature of the interaction. However, the electronegativity of heteroatoms and their geometric arrangements on the molecular rings shape electron-density distribution significantly differently for the three molecules. This difference gives rise to differences in competition and selectivity of reaction channels of these molecules. Isoxazole chemisorbs on Si(111)-7 \times 7 at 100 K through both dative-bond addition and [4 + 2]-like cycloaddition. Oxazole can be chemically attached to Si(111)-7 \times 7 through both dative-bond addition and [2 + 2]-like cycloaddition. The [2 + 2]-like cycloadduct is possibly partially thermally converted into a [4 + 2]-like cycloadduct. Thiazole chemisorbs on Si(111)-7 \times 7 at 100 K through formation of a dative-bonded adduct. The dative-bonded adduct is thermally converted into a [4 + 2]-like cycloadduct in the temperature range of 100–250 K. These studies for the three aromatic molecules with two different heteroatoms and the analysis for simple five-membered and six-membered aromatic molecules containing one heteroatom demonstrate that the surface chemistry of aromatic molecules is dominated by the distribution of molecular electron density, polarity, contribution of heteroatoms for formation of the aromatic conjugation of $(4n + 2)$ π electrons, geometric arrangement, and electronegativity of the heteroatoms on the aromatic ring.

Acknowledgment. This research was partially supported by the Chemistry Division of the National Science Foundation.

Supporting Information Available: Detailed assignment of the [4 + 2]-like cycloadduct formed from isoxazole. This material is available free of charge via the Internet at <http://pubs.acs.org>.

JA070182Y